ADVANCED TISSUE ANALYSIS AND DISPLAY WITH ULTRASOUND

J. F. Greenleaf, K. Chandrasekaran, and H. A. McCann

ABSTRACT--Computer-assisted imaging with ultrasound is shown to be useful for basic tissue characterization in ischemic heart studies, high-resolution imaging in tissue, and multidimensional imaging. Methods described include transmission tomography, backscatter tomography, coherent macrotomography, and volumetric multidimensional imaging.

In attempting to use ultrasonic energy for diagnostic imaging, one must discern those relationships between the tissue and propagating ultrasonic wave, which are sensitive to disease processes. There have been many attempts at relating quantitative properties of images of tissue obtained using ultrasound with disease properties [Carson et al., 1981; Glover and Sharp, 1977; Goss et al., 1978; Chandrasekaran et al., 1986]. In this paper we discuss the use of three types of imaging with ultrasound for characterizing tissue properties. All three techniques use computer-assisted analysis resulting in either quantitative images or qualitative images of the object. The first section of the paper is a rather heuristic description of ultrasonic scattering using graphical methods of depicting the scattering process that have been described elsewhere [Greenleaf, 1986]. The second section describes three methods in which computer analysis of scattering theory is used to analyze tissue depending on the specific geometries of the experiment involved. The final section is a discussion of possible future applications of computer-assisted ultrasonic imagery.

Scattering of Ultrasound

Let us consider an experiment described in Figure 1 in which an object is insonified with a transducer that produces a plane wave insonification. On the other side of the transducer, we receive the scattered energy with a hydrophone that is very small relative to the detail in the scattered wave. The relationship between the energy scattered by the object and the properties of the object itself, that is, the scattering function, can be considered to be a Fourier transform relationship [Greenleaf, 1986]. Figure 2 illustrates Fourier relationships between the measured transmitted scattered sound and the insonifying plane wave. One can see that the scattered wave measured by the scattering transducer is related to a circle in the Fourier space centered on the wave vector ($\bar{k}$) of the insonifying beam. The scattered energy is measured on a circle in the Fourier space as shown in the figure. Therefore, by rotating the insonifying wave around the object and measuring the scattering, the shaded portion of the Fourier transform of the object scattering function can be accessed.

In an experiment geometry in which the backscattered wave is measured, the receiving transducer of Figure 1 would be placed on the same side of the object as the insonifying wave. This allows a different part of the Fourier transform of the object to be accessed as shown in Figure 3. In this case, one sees that the portion of the circle accessed by backscattered waves is different from the portion of the scattering circle accessed by the forward scattering wave. By rotating the insonifying beam and associated backscatter receiver around the object, one can access data relating to the annular portion of the Fourier transform of the scattering function of the object.

Biodynamics Research Unit, Mayo Clinic and Foundation, Rochester, MN 55905 U.S.A.

///Trabalho recebido em 14/09/87 e aceito em 18/09/87///

This is depicted by the shaded portion of Figure 3. It is clear from these relationships that only a portion of the total Fourier transform of an object can be accessed by ultrasound and that that portion depends on the orientation of the ultrasonic energy and on the frequency of the energy.

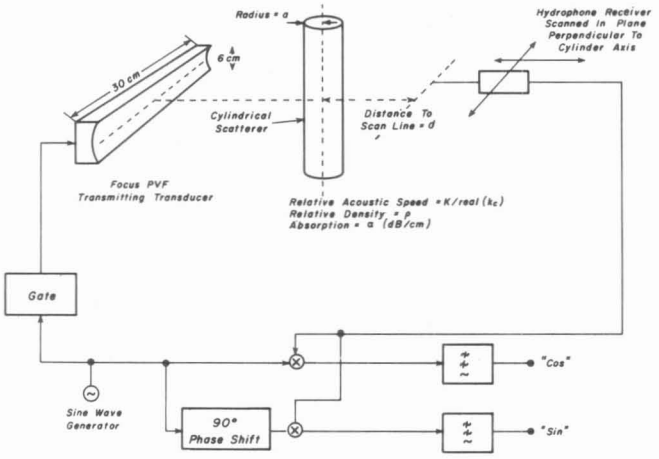

Figure 1 Experimental set up for scattering described by Figures 2 and 3. Plane wave insonification scatters off of object. Scattered energy is measured by hydrophone. (Reproduced with permission from B. Robinson and J. F. Greenleaf, *Acoustical Imaging*. New York, Plenum Publishing Corporation, 1984, 13, pp 163-178)

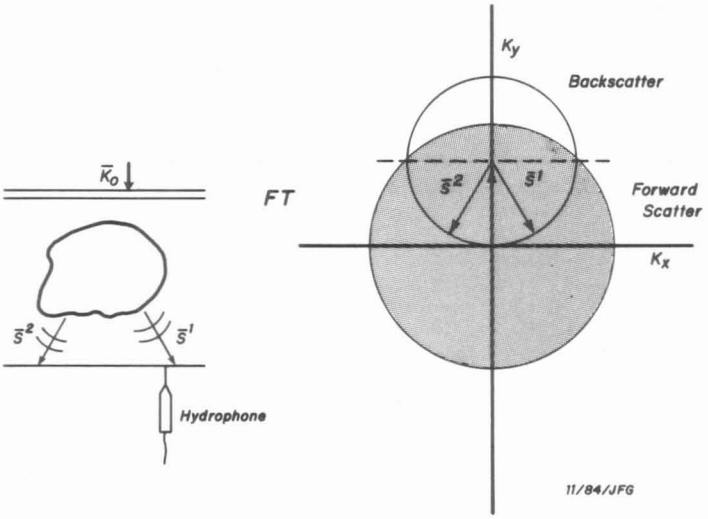

Figure 2 The scattered energy in the far field is related to the Fourier transform of the scattering function. In the forward geometry the interior circle of radius $\sqrt{2}\ K_o$ can be accessed. (Reproduced with permission from J. F. Greenleaf, 1984 IEEE Ultrasonic Symposium Proceedings 84CH2112-1 2(2):821-826, 1984)

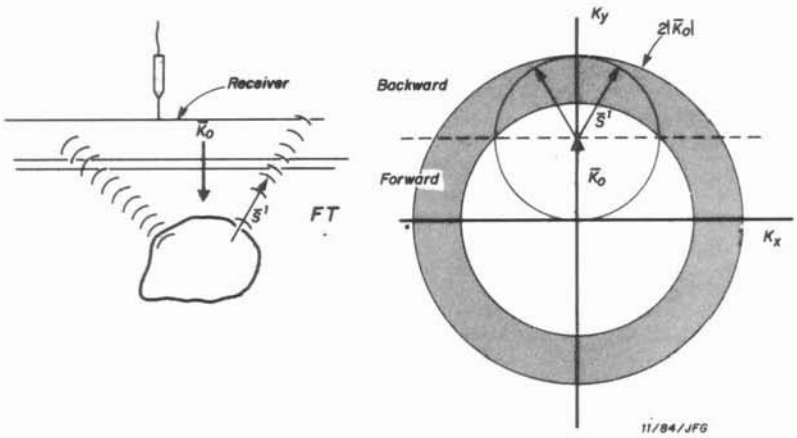

Figure 3 Backscatter geometry and associated relationship of scattering to the Fourier transform. The annulus from $\sqrt{2}$ K_o to 2 K_o is available in this geometry. (Reproduced with permission from J. F. Greenleaf, 1984 IEEE Ultrasonic Symposium Proceedings 84CH2112-1 2(2):821-826, 1984)

Parallel Transmission Tomography with Ultrasound

Figure 4 illustrates the geometry for typical ultrasonic transmission tomography. This type of tomography is characterized by two transducers scanning on either side of the object. The transmitter scans on one side while the receiver scans on the other side. By scanning across the object, a profile is obtained and under assumptions of parallel propagation of the wave. A set of these profiles for many orientation angles can be used to reconstruct an image representing the distribution of various properties of the object. If variations in signal amplitude are measured, a reconstruction of attenuation can be made and if variations in arrival time are measured reconstruction of an image representing speed of sound can be made of the insonified plane through the object. A laboratory set up is shown in Figure 5 in which transducers on each side of an excised heart are scanned back and forth in translate/rotate fashion obtaining transmission and reflection data required for computed tomography of the distribution of backscatter, attenuation, and speed.

This technique was used to study effects of experimental ischemia. Myocardial ischemia was produced in dog hearts by tying off the left anterior descending coronary artery for various periods of time. The hearts were then quickly excised and scanned in the bath as shown in Figure 5. The resulting images are shown in Figure 6. In these images of backscatter tomography, one can see regions of increased backscatter in the apical portion of the heart which are associated with ischemia while in the basal portion of the heart which contained normal perfusion, backscatter is low within the myocardium. Figure 7 illustrates a set of backscatter, transmission speed and transmission attenuation tomograms of the normal excised heart. By placing windows in regions of these tomograms of the excised hearts and measuring the speed, attenuation, and backscatter for the different regions of dog hearts that had undergone various lengths of time of ischemia prior to excision of heart, we obtained the data for Figure 8. Using these techniques for analyzing the distribution of attenuation, speed, and backscatter, we found that the backscatter increases with ischemia, the attenuation decreases, and the speed of sound decreases (Figure 8). These findings are consistent with increased edema within the tissue causing increased scattering by separation of the scattering elements (myofibrils) and

making the scattering more heterogeneous while the increased edema diluted the protein concentration, the principal cause of absorption, causing a decrease in attenuation and also decreased speed of sound toward that of water.

Analysis of backscatter in an open-chested heart [Chandrasekaran et al., 1987] resulted in variations in backscattered energy as a function of the cardiac cycle, represented by the electrocardiogram as shown in Figure 9 One can see that the backscatter in the normal region decreases with systole and increases with diastole while the backscattering in the ischemic region is relatively constant and higher than the normal region. This result is in keeping with the findings of others [Miller and Sobel, 1982; Miller et al., 1976].

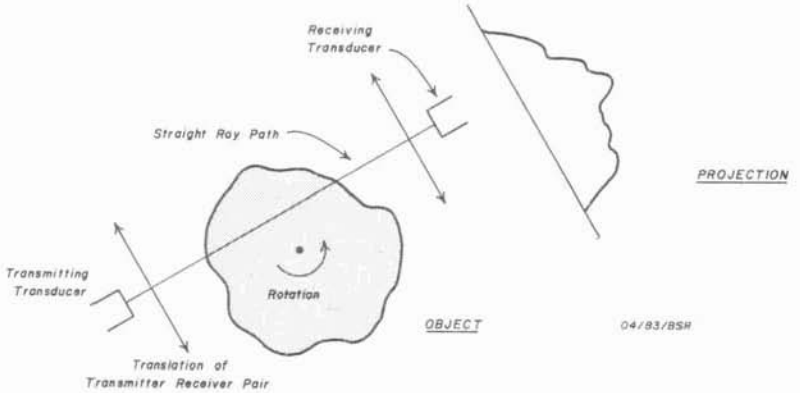

Figure 4 Geometry for transmission computed ultrasound tomography. The path of ultrasound is assumed to be straight. Parallel reconstruction can be done in this geometry if there is not too much diffraction or refraction. (Reproduced with permission from B. S. Robinson and J. F. Greenleaf, *Three-Dimensional Biomedical Imaging*. CRC Press, Boca Raton, FL, 1985, Volume II, pp 57-78)

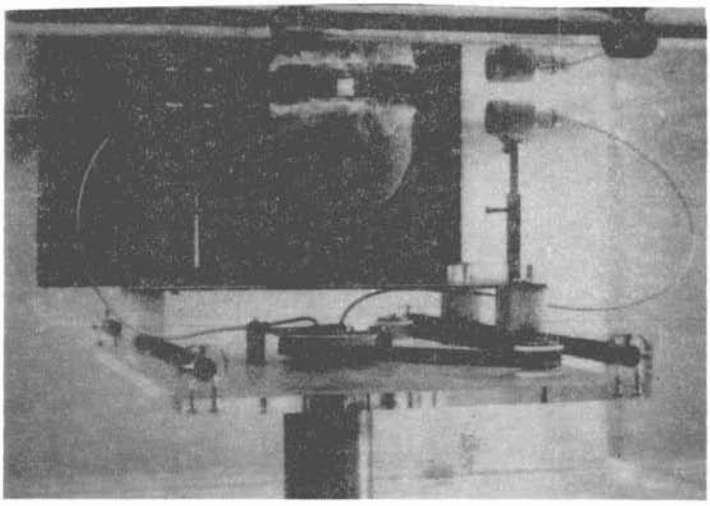

Figure 5 Experimental set up for measurement of backscatter, attenuation, and speed within freshly excised canine heart used in ischemia experiment. (Reproduced with permission from Chandrasekaran et al., 1986)

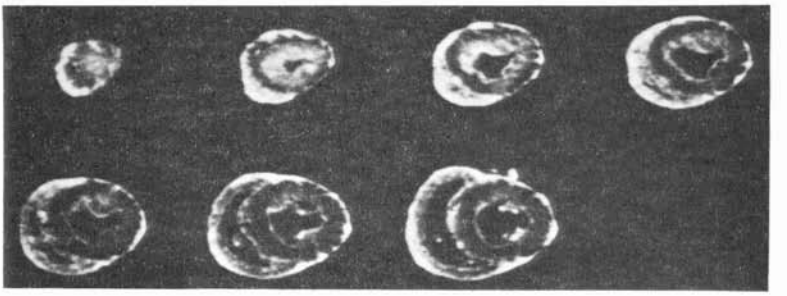

Figure 6 Computed backscatter images of planes through canine heart. Bright endocardial regions near apex show increased backscatter due to edema secondary to ischemia. (Reproduced with permission from Chandrasekaran et al., 1986)

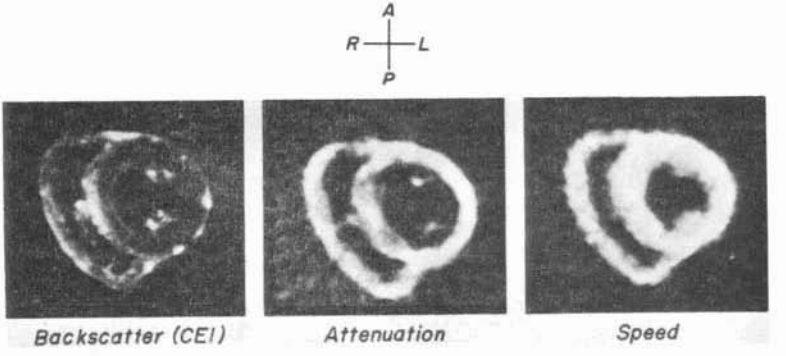

Figure 7 Sample set of backscatter, speed, and attenuation images that were analyzed to obtain data for Figure 8.

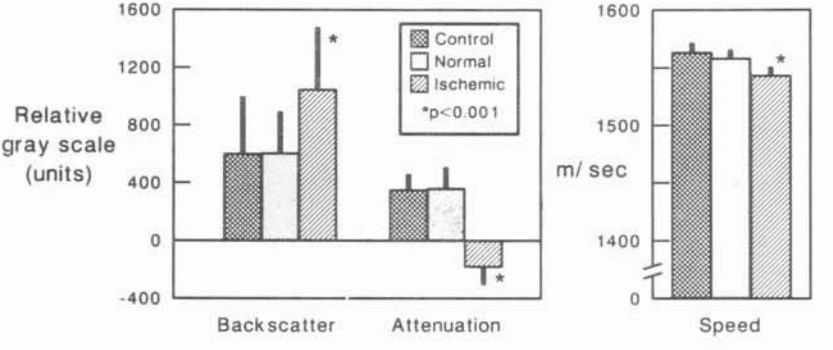

Figure 8 Comparison of normal and ischemic values of backscatter, speed, and attenuation.

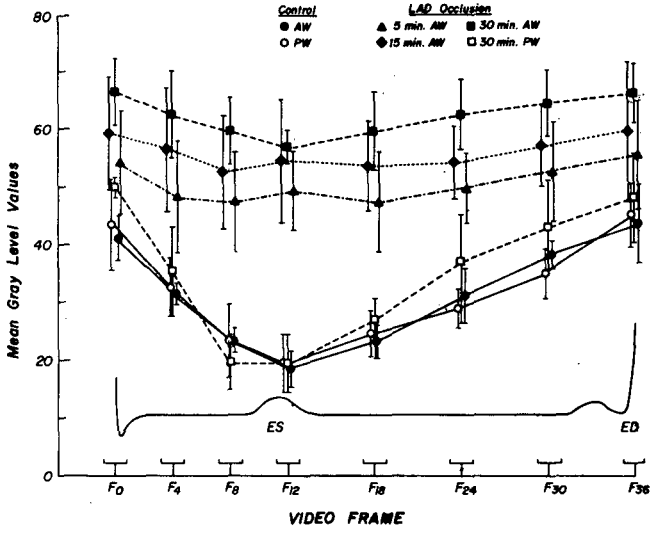

Figure 9 Variations of backscatter vs. time in normal (open) and ischemic (filled) hearts. Twelve MHz transducer on open-chested heart. (Reproduced with permission from Chandrasekaran et al., 1987)

Focused Macrotomography

We have developed a completely different type of tomography which can be accomplished in the backscatter mode deep within the tissue [Ylitalo et al., 1986; Ylitalo and Greenleaf, 1987]. Figure 10 illustrates this technique. A transducer is focused on a small region deep within the tissue and rotated around a center of rotation within that region. The resulting signal represents the projection of scatterers within the region since within the focal region of the transducer the wave is relatively plane over a length extending across the depth of field. If a large number of profiles are taken around a large angle of view, then these profiles can be reconstructed into an image of backscatter. Figure 11 illustrates a means by which the data are focused using this technique. One can imagine that variations in acoustic speed of tissue intervening between the region to be imaged shown in Figure 10 and the receiver will vary the arrival time of the 'profile', thus causing blurring of the resulting reconstruction. A technique has been developed for focusing the transducer [Ylitalo, 1987] in which the arrival times are fit to a best sinusoid, thus tending to focus the image. The result of such focusing is shown in Figure 12 in which the right image is the compound B-scan which would typically be obtained from the data obtained in this scan and the left image is the focused coherent tomoscan in a piece of liver. This experiment was conducted on excised tissues and has not yet been done *in vivo*.

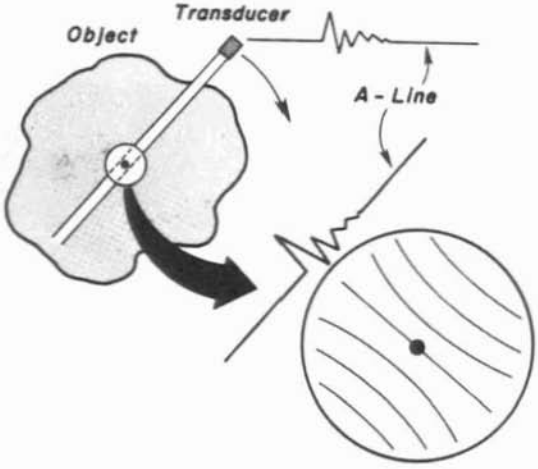

Figure 10 In focal region of transducer the waves are nearly plane and parallel. Thus an A-line in this region represents projections of the scatterers along the beam direction. These 'profiles' can be used to reconstruct images of the region. (Reproduced with permission from J. F. Greenleaf, J. Ylitalo, and J. J. Gisvold, IEEE Engineering in Medicine and Biology Magazine (In Press))

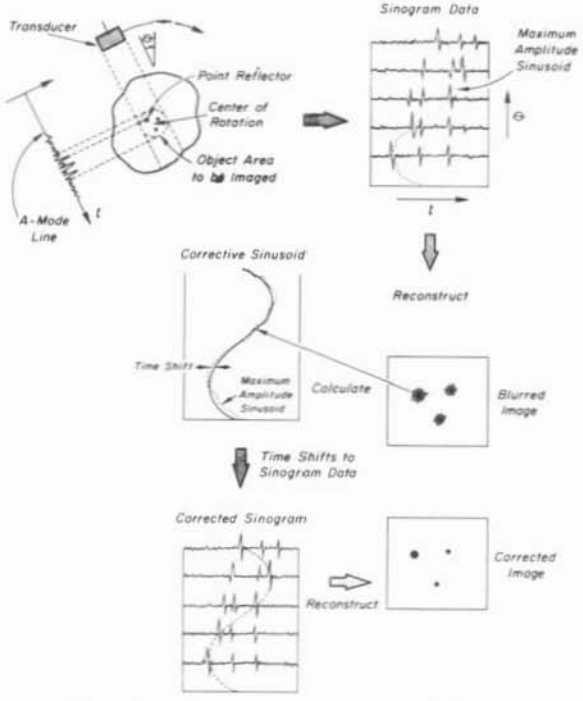

Figure 11 Means of focusing macrotomography. A bright sinusoid in the Radon transform of the image is adjusted for variations in arrival time. The resulting data

are reconstructed into a focused image. (Reproduced with permission from Ylitalo and Greenleaf, 1987)

Figure 12 Focused macrotomogram (left) compared to a compound B-scan (right) of the same region of excised liver tissue. (Reproduced with permission from Ylitalo, 1987)

Computer-Assisted Multidimensional Imaging

The development of three-dimensional images of the beating heart has been frustrated in the past by the inability to acquire enough data to characterize this complex, time varying structure. We have recently developed techniques for obtaining data utilizing a conventional clinical ultrasound scanner. By rotating the sector scanner around its central beam and digitizing a sequence of fifty B-scan images at the same point in the cardiac cycle separated by 3.6°, we have obtained enough data for high-fidelity multidimensional images of the heart. Figure 13 describes the mechanism by which the data are acquired. By recording the B-scan of the heart at fifty separate views throughout several cycles of the heart, one can post priori select images at each view associated with a single point in the cardiac cycle. Lines from each view are selected and interpolated into a plane within a three-dimensional volume depicting the heart or region of the heart under examination. The scanner is fixed to the thorax of the patient using locking universal joints which are connected to a thermoplastic frame wrapped around the patient's chest as shown in Figure 14.

Using an advanced multidimensional data analysis package, ANALYZE, developed over the past ten years in the Biodynamics Research Unit of the Mayo Clinic [Robb et al., 1986], the volumetric data produced by multidimensional scanning of the heart can be analyzed in detail. Figure 15 illustrates a method of sectioning the volume image in an oblique section for analysis of views of the heart not available with conventional two-dimensional ultrasonic echocardiography. The set of backscattered data digitized from the echocardiographic images can be selected for various regions of the heart, such as the left ventricle, and reprojected for viewing at various angles as shown in Figure 16. The anterior surfaces of the backscattered distributions can be detected by semi-automated surface detection and resulting surfaces can be shaded to depict the left ventricle and outflow tract at diastole and systole as shown in Figure 17. Therefore, dynamic images of the heart can be made in which various components of the myocardium or ventricular chambers can be evaluated and their relationships with time or perhaps clinical interventions can be studied [McCann et al., 1987].

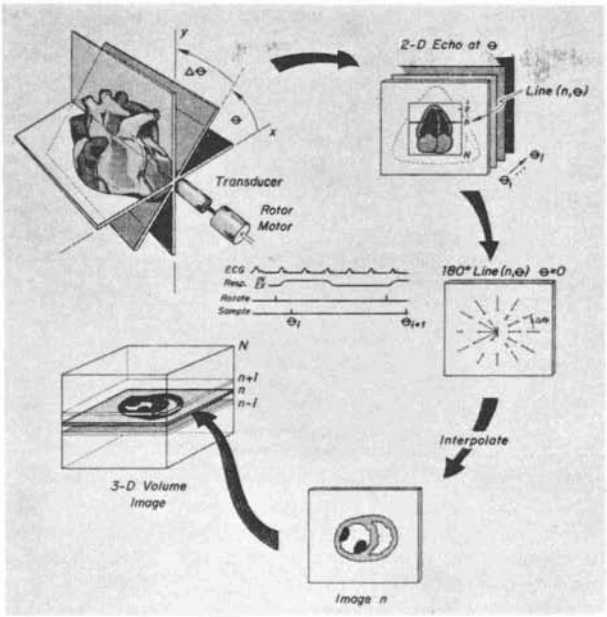

Figure 13 Data flow diagram for multidimensional heart imaging. About 50 angles of view are digitized and interpolated into a planar image. The resulting stack of images represents the distribution of backscatter measured in the heart volume. (Reproduced with permission from McCann et al., 1987)

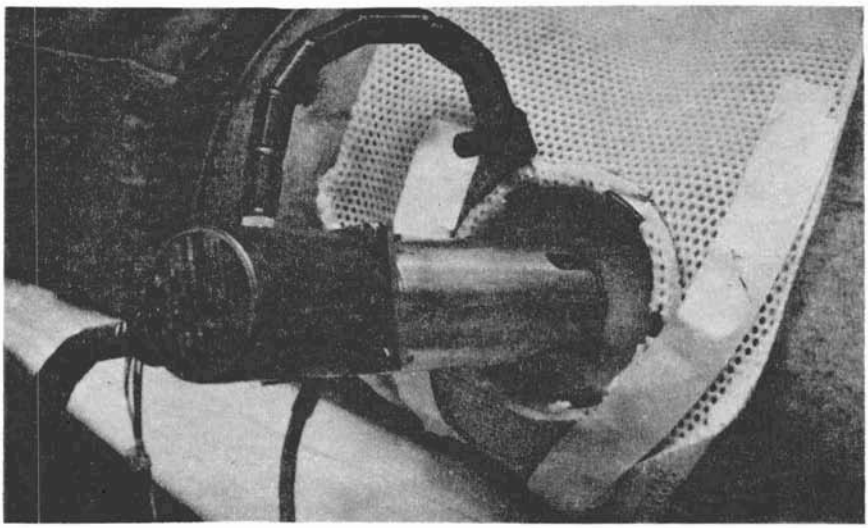

Figure 14 Thermosetting plastic cast and locking universal joints used to stabilize the scanner and rotating stepper motor relative to the thorax. (Reproduced with permission from McCann et al., 1987)

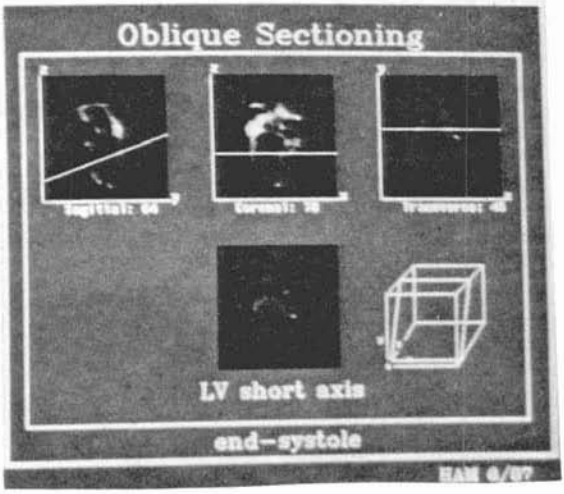

Figure 15 Sections of the volume of data can be analyzed at oblique angles. Views not available with conventional B-scans can be obtained. (Reproduced with permission from McCann et al., 1987)

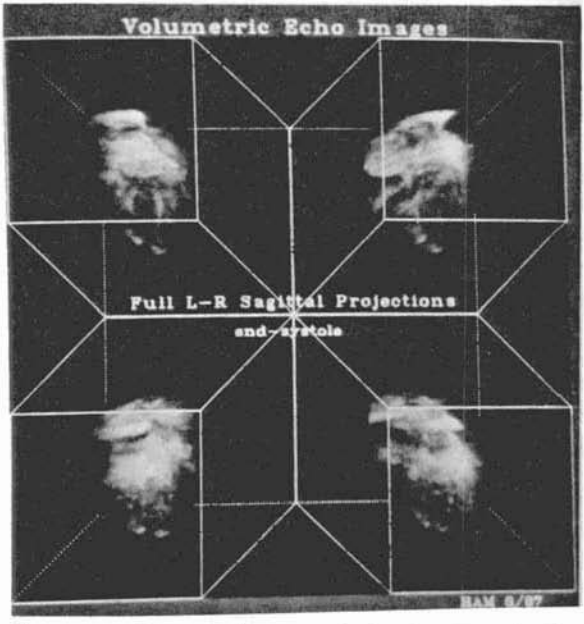

Figure 16 Backscatter volumetric images of the heart made from four different viewpoints. (Reproduced with permission from McCann et al., 1987)

Figure 17 Surfaces of the left ventricle of a volunteer obtained by semi-automated surface detection. Four views separated by 90° of diastole (upper) and systole (lower) illustrate the left ventricular chamber and outflow track. (Reproduced with permission from McCann et al., 1987)

Future Possibilities for Ultrasonic Imaging

One can imagine that a wide range of data will in the future be acquired from patients and analyzed at advanced workstations by highly-trained medical imaging specialists. These workstations would allow analysis of multidimensional data so that dynamic parameters such as volume, filling and ejection characteristics and wall stress could be studied as well as specific views of the organs unavailable with current imaging technology. As computers become faster and have larger memories, these analyses will become simpler and very easily done so that complete analyses of the various organ systems being evaluated can be accomplished in a short time.

Acknowledgments

This work was supported in part by grants CA 24085, HL-07111, CA 36029, HL-04664, and RR-02540 from the National Institutes of Health. The authors wish to thank E. C. Quarve for and S. D. Orwoll for secretarial assistant and graphics. The authors wish to thank E. A. Hoffman for advice on volumetric imaging with ANALYZE.

References

Carson, P. L., C. R. Meyer, A. L. Scherzinger, and T. V. Oughton: Breast imaging in coronal planes with simultaneous pulse echo and transmission ultrasound. Science 214:1141-1143, 1981.

Chandrasekaran, K., J. F. Greenleaf, K. H. Kim, W. D. Edwards, J. B. Seward, and A. J. Tajik: Epicardial echocardiography in tissue characterization of ischemic myocardium in a canine model. American Journal of Cardiac Imaging 1(2):152-159, 1987.

Chandrasekaran, K., J. F. Greenleaf, B. S. Robinson, W. D. Edwards, J. B. Seward, and A. J. Tajik: Echocardiographic visualization of acute myocardial ischemia--*in vitro* study. Ultrasound in Medicine and Biology 12(10:785-793, 1986.

Glover, G. H. and J. C. Sharp: Reconstruction of ultrasound propagation speed distribution in soft tissue: Time-of-flight tomography. IEEE Transactions on Sonics and Ultrasonics SU-24(4):229-234, 1977.

Goss, S. A., R. L. Johnston, and F. Dunn: Comprehensive compilation of empirical ultrasonic properties of mammalian tissues. Journal of the Acoustical Society of America 64(2):423-457, 1978.

Greenleaf, J. F.: A graphical description of scattering. Ultrasound in Medicine and Biology 12(8):603-609, 1986.

McCann, H. A., K. Chandrasekaran, E. A. Hoffman, L. J. Sinak, T. M. Kinter, and J. F. Greenleaf: A method for three-dimensional ultrasonic imaging of the heart *in vivo*. Cardiovascular Dynamics (In Press).

Miller, J. B., D. E. Juhas, J. W. Mimbs, S. B. Dierker, L. J. Busse, J. J. Laterra, A. N. Weiss, and B. E. Sobel: Ultrasonic tissue characterization: Correlation between biochemical and ultrasonic indices of myocardial injury. 1976 Ultrasonics Symposium Proceedings, Catalog #76, 1976.

Miller, J. G. and B. E. Sobel: Cardiac ultrasonic tissue characterization. Hospital Practice, pp 143-151, January, 1982.

Robb, R. A., P. B. Heffernan, J. J. Camp, and D. P. Hanson: A workstation for interactive display and quantitative analysis of 3-D and 4-D biomedical images. IEEE Computer Applications in Medical Care 1986, October 25-26, 1986, Washington, DC, pp 240-256, 1986.

Ylitalo, J.: Coherent high-resolution ultrasound reflection mode CT imaging, University of Oulu, Oulu, Finland (Thesis), 1987.

Ylitalo, J. and J. F. Greenleaf: A correction method for speed variations in high-resolution ultrasound reflection mode CT imaging. In: K. Toda: *Ultrasonic Technology 1987*, Toyohashi International Conference on Ultrasonic Technology, Toyohashi, Japan, MYU Research, 1987, pp 55-62.

Ylitalo, J., J. F. Greenleaf, and R. C. Bahn: Coherent high-resolution ultrasound reflection mode CT imaging. 1986 IEEE Ultrasonics Symposium 833-841, 1986.